Tree Breakage Characteristics Under Static Loading -- Ponderosa Pine

Interim Technical Report AFSWP-406

CONFIDENTIAL

Interim Technical Report
AFSWP - 406
January 15, 1953

Declassified July 5, 1957 Ltr from AFSWP

TREE BREAKAGE CHARACTERISTICS UNDER STATIC LOADING

PONDEROSA PINE

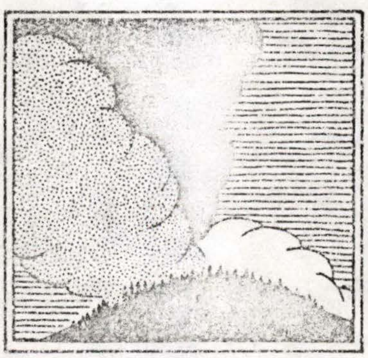

DIVISION OF FIRE RESEARCH
FOREST SERVICE
U. S. DEPARTMENT OF AGRICULTURE

Declassified July 5, 1957 Ltr from AFSWP

CONFIDENTIAL

TREE BREAKAGE CHARACTERISTICS UNDER STATIC LOADING

PONDEROSA PINE

by

W. L. Fons

U. S. Department of Agriculture
Forest Service
Division of Fire Research

A. A. Brown, Division Chief

January 15, 1953

Interim Technical Report 406
for the
Armed Forces Special Weapons Project
Washington, D. C.

This study is part of a group research project of the Division of Fire Research, Forest Service, U. S. Department of Agriculture, conducted at the California Forest and Range Experiment Station.

W. L. Fons was responsible for this work with technical corroboration and checking by F. M. Sauer. V. M. DeKalb and O. Brichacek supervised field work. T.G. Storey made statistical analyses and supervised computations. W. Lai drafted illustrations.

Keith Arnold, Project Leader

CONTENTS

ILLUSTRATIONS

TABLES

CHAPTER 1

INTRODUCTION

Historical

Determination of tree breakage characteristics for ponderosa pine is one of a number of studies aimed towards developing a system which predicts blast damage to roadside and forest trees from atomic explosions.

Blast damage to trees is primarily a function of aerodynamic drag of tree crowns and the force and deflection characteristics of tree stems. In assessing blast damage to forest stands, consideration must also be given to the effect of those stands on attenuation of blast winds.

Previous work has shown that aerodynamic drag of tree crowns in a steady wind is correlated with dry weight of crown. [1] Preliminary analysis employed a single-mass, spring-mass system to establish significant tree-characteristic parameters and shock-wave characteristics which affect the probability of breakage and blow-down following atomic explosions. Breakage predictions made from this analysis were field checked in Operation SNAPPER. [2]

The present study was initiated to determine the force and deflection necessary to break naturally rooted tree stems under static loading.

Summary

Static bending tests were made on 25 pine-tree stems selected for apparent soundness and lack of visible defect. These stems, which varied in diameter from 10 to 32 in. and in height from 33 to 124 ft, were loaded by a cable attached to a preselected loading point until they failed. Measurements of deflection and force were made at the point of failure and at 2- to 3-ft intervals during bending prior to failure.

---

1 U. S. Dept. of Agriculture, Forest Service, Division of Fire Research. Experimental Investigation of Aerodynamic Drag in Tree Crowns Exposed to Steady Wind--Conifers. Phase Report for Operations Research Office. December 20, 1951, 19 pp. (CONFIDENTIAL Security Information)

2 Forest Service, A.F.S.W.P. Operation SNAPPER Final Report, Project 3.3. December 1, 1952. (CONFIDENTIAL Security Information--RESTRICTED DATA)

Tree stem dimensions, stem form, and position of loading on the stem were determined to be the critical parameters characterizing force and deflection phenomena. Application of small-deflection theory to these parameters provided: (1) quantitative estimates of stress distribution along the stem for different points of loading; (2) equations from which the approximate location of the break along the stem could be predicted; and (3) a method of predicting force and deflection at breakage. This analysis was used to correlate experimental data from the static bending tests.

Variations in the order of 300 per cent in observed force and deflection required to break apparently similar trees made it necessary to establish probability curves for these breakage characteristics for field application. Average calculated stress of position of stem breakage was 70 per cent of the modulus of rupture determined by standard tests on green sawed specimens of the same species. The fact that none of the trees uprooted is attributed to characteristic wide-spreading lateral roots of ponderosa and loblolly pine and to low soil-moisture conditions.

CHAPTER 2

ANALYSIS

Theoretical specification of the forces required and the large relative deflections associated with tree-stem breakage under static loading involves solution of a nonlinear second-order differential equation. This problem is further complicated by elastic-plastic deformation at high stress, by inherent stress concentrations, nonuniformity of the tree stem, and variations in mechanical properties of the wood itself.

The following analysis, based on small deflection theory, delineates essential parameters concerning the problem of stem breakage due to a single load. These parameters present a basis for the correlation of experimental stem breakage data. This analysis also provides quantitative estimates of stress distribution along the stem for different points of loading and prediction of probable position of failure.

Stress Along Stem

Measurements of cross sections of coniferous tree stems by Behre [3] have shown that the stem form may be represented by

$$z = \frac{f}{af + b} \qquad (2.1)$$ [4]

where a and b are constants.

The tree stem is considered to be a homogeneous cantilever beam of circular cross section which is fixed or rigid at breast height. [5] Since root swell is usually pronounced up to breast height this assumption of no bending below that point should not seriously affect prediction of deflections in the upper part of the tree stem.

The compressive or tensile unit stress due to loading is determined by the flexure formula

---

3/ C. Edward Behre. "Form-Class Taper Curves and Volume Tables and Their Application," Journal of Agricultural Research, XXXV (October 1927), 673-744.

4/ Nomenclature given on page 45.

5/ Breast height is 4 1/2 ft above ground level.

$$M = \frac{sI}{C} \tag{2.2}$$

Since bark is not considered to contribute to stem strength, the moment of inertia is determined from stem diameter inside bark. Variation of moment of inertia due to stem taper is given by the equation

$$I = I_{bh} \left(\frac{d}{d_{bh}}\right)^4 \tag{2.3}$$

Stress along the stem due to a single horizontal force, R, applied at some fractional distance, f_1, from top of stem (Fig. 2.1) is obtained by combining Equations 2.1, 2.2, and 2.3

$$\frac{s}{s_{bh}} = \frac{f - f_1}{1 - f_1} \left[\frac{f + c}{f(1 + c)}\right]^3 \tag{2.4}$$

where $s_{bh} = \frac{32RH_{bh}}{\pi d_i^3} (1 - f_1)$, the stress at $f = 1$.

Position of maxima in the stress distribution curve may be determined by differentiating Equation 2.4 with respect to f and letting $ds/df = 0$. Maximum stress occurs at

$$f_m = c \pm (c^2 - 3cf_1)^{1/2} \tag{2.5}$$

with the signs (-) for $c > 0$ and (+) for $c < 0$.

Force Deflection

In the region where deflection is proportional to applied force, the theoretical restoring force constant is

$$k_r = \frac{R}{y(f_1)} \tag{2.6}$$

For small deflections the expression for stem deflection may be obtained from the elastic curve equation

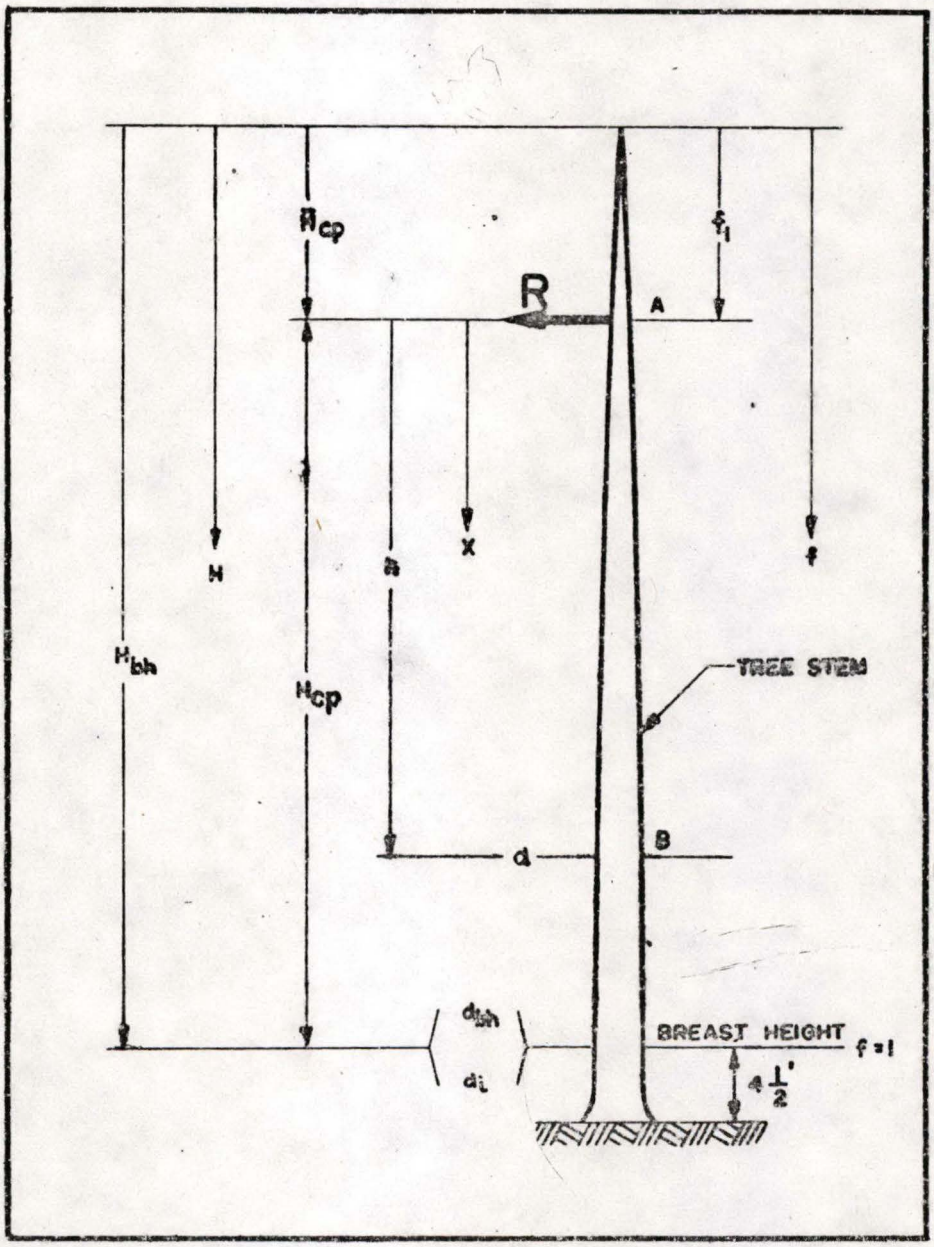

Fig. 2.1 Schematic Diagram Showing Tree Stem and Associated Parameters

$$\frac{d^2y}{dx^2} = \frac{Rx}{EI} \tag{2.7}$$

where x is the distance along the stem measured from the point of force application downward (Fig. 2.1) and is expressed as

$$x = H_{bh}(f - f_1) \tag{2.8}$$

Substituting Equations 2.3 and 2.8 in Equation 2.7, and performing the necessary integration [6] produces the expression for deflection

$$y = \frac{RH_{bh}^3}{3EI_i} \phi(c, f_1, f) \tag{2.9}$$

Letting $y = y(f_1)$ in Equation 2.9 and combining with Equation 2.6 yields a dimensionless expression containing the restoring force constant

$$\frac{k_r H_{bh}^3}{3EI_i} = \psi(c, f_1) \tag{2.10}$$

Equation 2.10 is shown graphically in Fig. 2.2 for applicable ranges of c and f_1.

Strain Deflection

In the elastic region the normal unit-stress in the material is equal to the modulus of elasticity times the unit-strain in the direction of the stress

$$s = E\delta \tag{2.11}$$

Substituting Equation 2.11 in Equation 2.2

$$\delta = \frac{MC}{EI} \tag{2.12}$$

[6] Appendix A presents complete derivations.

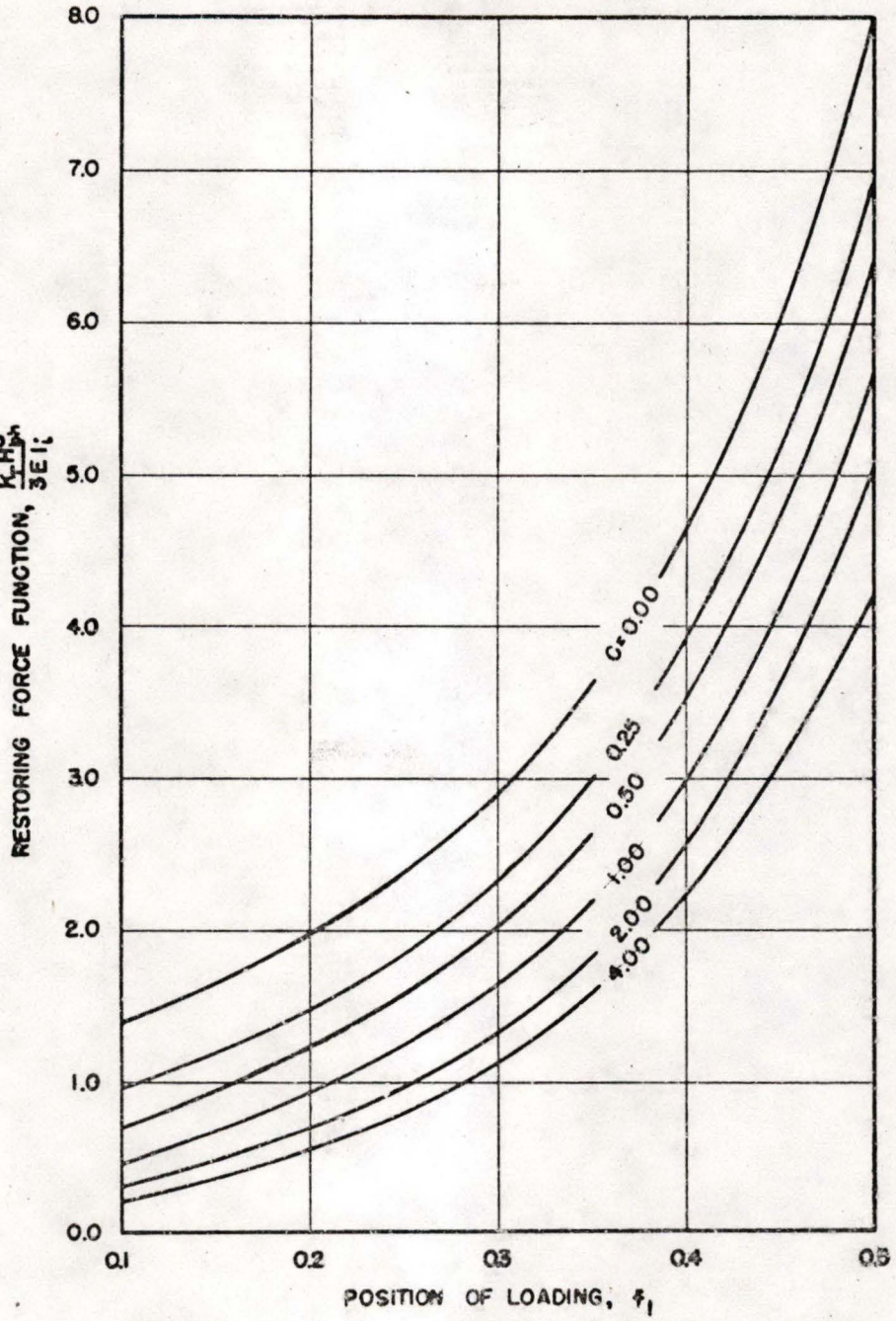

Fig. 2.2 Dimensionless Expression Containing Restoring Force Constant, k_r, as a Function of Position of Loading, f_1, and Stem Form Factor, c

By considering that loading is at point A, Fig. 2.1, Equation 2.12 for strain at point B is

$$\delta = \frac{Rhd}{2EI}$$

or

$$\delta = \frac{k_r hd}{2EI} \; y \tag{2.13}$$

Substituting for k_r from Equation 2.10 in 2.13 gives

$$\delta = \left[\frac{3hd}{2H_{bh}^3} \left(\frac{d_i}{d} \right)^4 \psi (c, f_1) \right] y(f_1) \tag{2.14}$$

Equation 2.14 indicates that strain is directly proportional to deflection. Parameters in the bracket remain constant, and the quantity is the slope of line δ as a function of $y(f_1)$.

The maximum strain corresponding to deflection at f_1 is

$$\delta_m = \left[\frac{3d_i(1 - f_1)}{2H_{bh}^2} \; \psi (c, f_1) \right] \frac{s_m}{s_{bh}} \; y(f_1) \tag{2.15}$$

CHAPTER 3

PROCEDURE

Static bending tests were made on 25 pine tree stems by pulling them with a cable attached to a preselected loading point until breakage occurred.

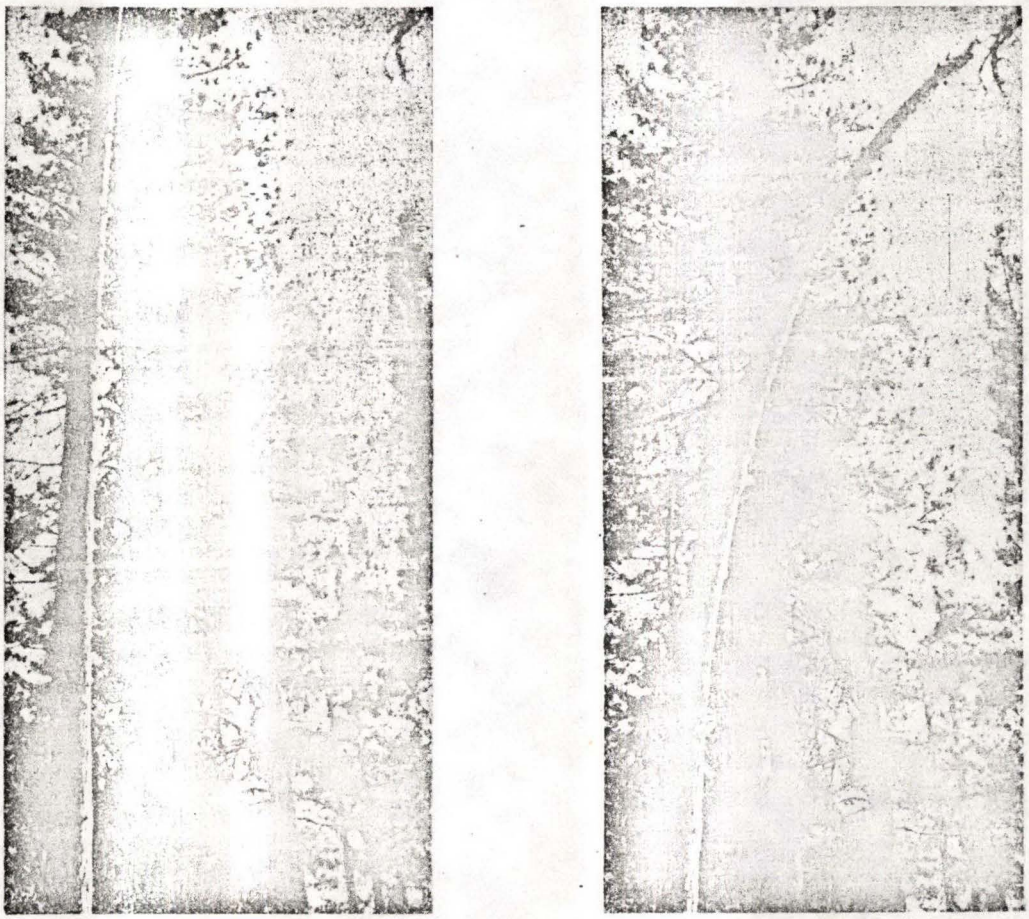

Fig. 3.1 Tree 12, Stanislaus National Forest, at 6 ft Deflection and 28 ft Deflection Just Prior to Breakage

Tree Selection

Sound trees with no defect visible from the ground, i. e. fire scar, rot, crook, or fork, were used for test specimens. Trees varied in diameter from 10 to 32 in. and in height from 33 to 124 feet. Table 3.1 describes site situations from which test trees were selected. All tests were conducted with dry soil conditions.

TABLE 3.1

Site Situations of Test Trees

Tree Numbers	Species	Location	Site	Crown Canopy Condition
1 - 5	Ponderosa pine	Shasta National Forest, Calif.; elevation 4,000 ft	I-II	Semi-open
6 - 9	Ponderosa pine *	Charleston Ranger District, Nevada National Forest, Nevada; elevation 8,000 ft	IV-V	Open
10 - 21	Ponderosa pine	Stanislaus National Forest, Calif.; elevation 4,000 ft	I-II	Semi-open
22 - 25	Loblolly pine	Santee Experimental Forest, South Carolina, elevation 300 ft		Closed

* These trees were transported to Nevada Proving Grounds, and the stems set rigidly in concrete.

Test Description

Total height, diameter breast high, and position of load application point were measured. Next the limbs were removed and the stem cut just above the point of loading in order to eliminate their weight influence on loading.

Figure 3.2 shows installation and location of: cable through which the load was applied; dynamometer and oscillograph recorder which measured force of the load applied; and transit used to record movement of point of loading. Loading was stopped at successive 2- to 3-ft deflections to record transit readings. Though 4 to 10 pairs of such readings

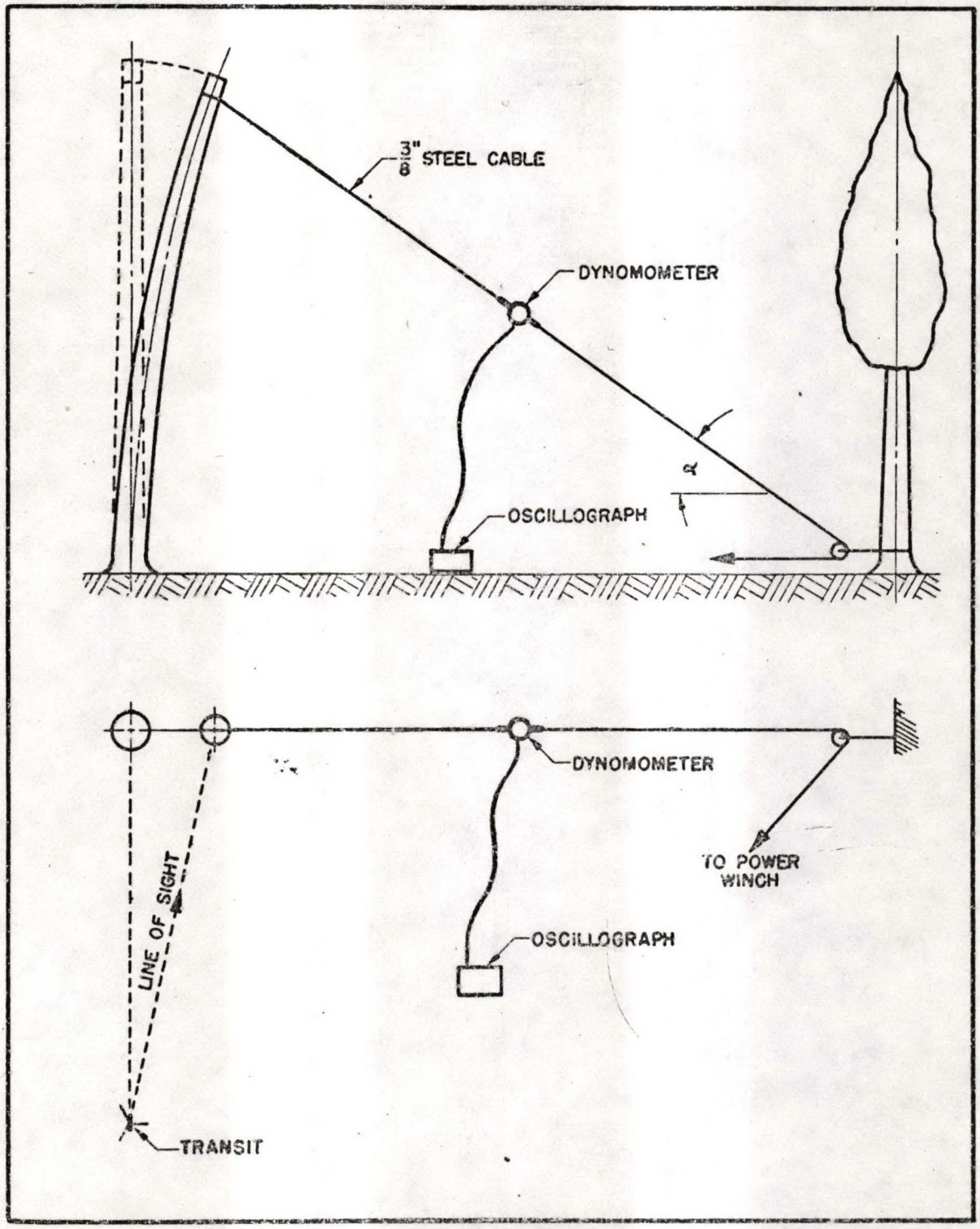

Fig. 3.2 Layout for Static Bending Tests

were taken, depending on total deflection, the transit operator had to follow the moving loading point constantly in order to catch its precise location when failure occurred. Layout of stem, block, and transit was sketched, and distances were measured.

Following stem failure the standing portion was cut 1 ft above the ground, position of break on the stem was measured, and characteristics of failure described. Cuts were made at 10-ft intervals along the stem and on each side of the break. Average diameters inside bark of each section were measured for determination of form factor.

Instrumentation

Loading of the ring dynamometer (Fig. 3.3) was measured by mounting four type A-5 SR-4 strain gages on opposite sides of the steel ring. Gages were connected to form adjacent arms of a four-element bridge circuit (Fig. 3.4). As the ring deflected under load, the resultant strain caused a change in the resistance in the gages, which in turn was recorded on a Sanborn 127 oscillograph equipped with a strain-gage amplifier. Power for the oscillograph was supplied from two 12-volt wet storage batteries through a 12-volt DC 110-volt AC synchronous converter.

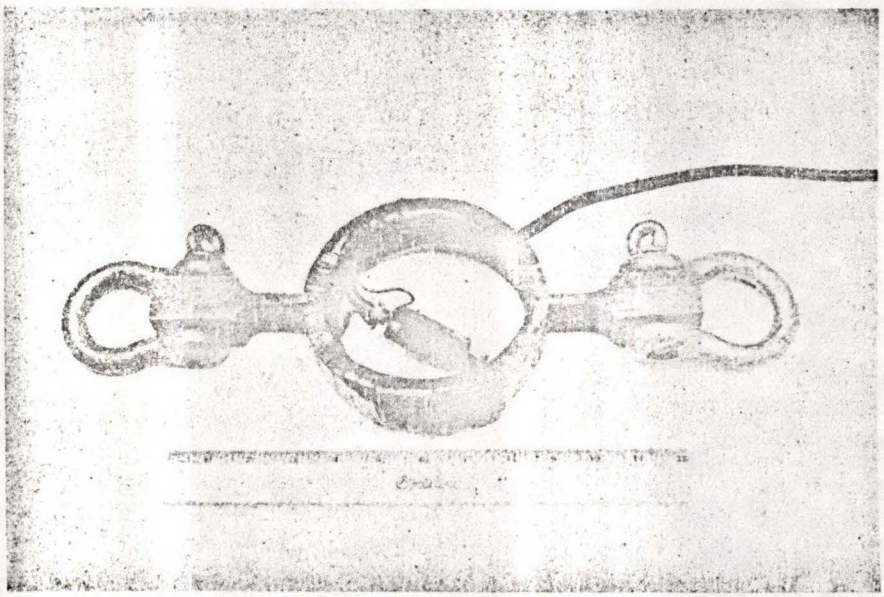

Fig. 3.3 Ring Dynamometer for Load Measurement

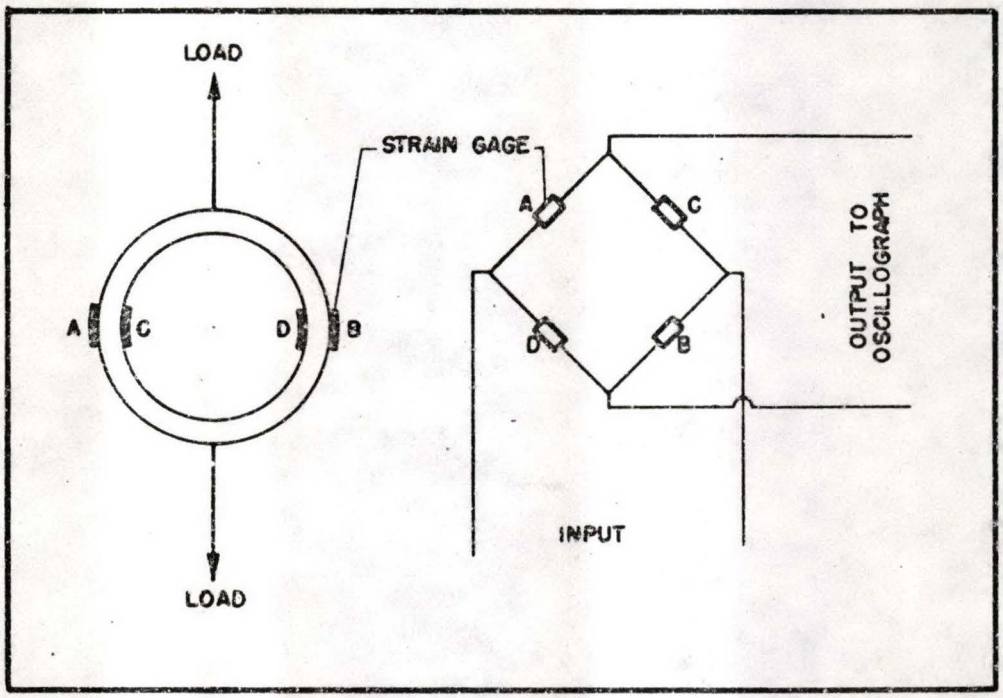

Fig. 3.4 Strain Gage Location and Ring Dynamometer Bridge Circuit

Calibration of the dynamometer (Fig. 3.5) made on a tensile testing machine at the conclusion of the experiments indicated an experimental constant of 63.5 compared to a theoretical constant of 65.6, which was calculated from the physical properties of the ring.

Horizontal and vertical transit angles to the point of loading were taken from a known transit location. These data were used to compute deflection of the tree stem for the correspondingly measured load.

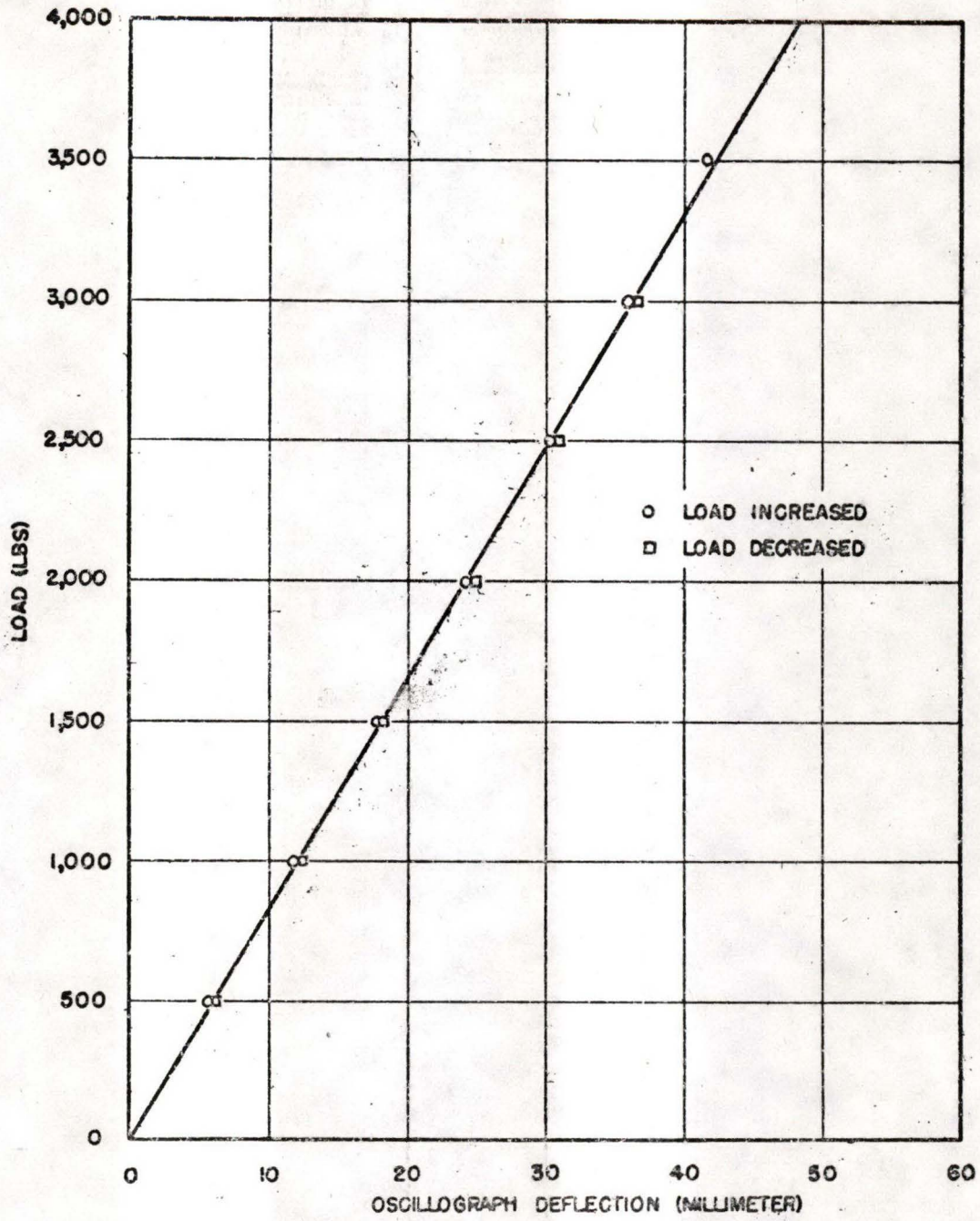

Fig. 3.5 Ring Dynamometer Calibration

CHAPTER 4

DATA AND RESULTS

Physical characteristics of each tree stem tested, horizontal force and deflection for breakage, and the positions of loading and breakage, are recorded in Table 4.1, page 22.

Mechanical properties used for computations were for green wood.7/

TABLE 4.2

Mechanical Properties of Green Wood

Species	Modulus of Elasticity, E (Lbs/Sq In.)	Modulus of Rupture, S (Lbs/Sq In.)	Reference Strain $\delta_r = \frac{S}{E}$ (In./In.)
Ponderosa pine	0.97×10^6	5,000	0.0051
Loblolly pine	1.41×10^6	7,300	0.0052

Figure 4.1 shows a typical force-deflection curve where arc deflections were determined from transit data by measuring along the locus of plotted points and corresponding horizontal force was found by multiplying measured force by cos α.8/

Values of constants "a" and "b" in Equation 2.1 were obtained from graphs drawn for each tree which are similar to Fig. 4.2. In drawing the straight line, more weight was given to those points where $f > f_1$.

Table 4.3 presents values of breakage parameters derived from data of Tables 4.1 and 4.2. The actual restoring force constant k_a for each stem was calculated from a value of force R and a corresponding value of deflection $y(f_1)$ in the elastic region (Fig. 4.1). Table 4.4 shows how the remaining parameters were calculated. Figure 4.3 presents the relation between $\bar{K}$ and $\bar{H}$.

7/ L.J. Markwardt and T.R.C. Wilson. Strength and Related Properties of Woods Grown in the United States. U.S. Dept. of Agriculture Tech. Bulletin 479. Washington: U.S. Govt. Printing Office, 1935.
8/ Force-deflection data for all trees tested are tabulated in Appendix B.

TABLE 4.1

Experimental Stem Breakage Data

Column	1	2	3	4	5	6	7	8	9	10	11	12
Tree No.*	Age (Yrs)	H_{bh} (Ft)	d_{bh} (In.)	d_i (In.)	H_{cp} (Ft)	f_1	b	a	c	R_b (Lbs)	$y_b(f_1)$ (Ft)	f_{br}
1	54	89.5	26.4	19.4	66.1	.26	.62	.79	.778	2450	24.5	.52
2	54	84.0	22.0	18.4	51.2	.39	.60	.60	1.000	2700	14.0	.84
3	72	124.5	32.5	25.4	76.5	.38	.70	.57	1.861	3900	20.0	.54
4	60	85.0	21.0	19.0	40.3	.53	.50	.83	0.604	3450	11.5	1.00
5	58	89.5	23.5	21.2	49.1	.45	.61	.52	1.173	2500	14.5	.80
6	140	34.2	11.3	9.4	26.4	.20	.55	.65	.846	1445	15.0	.68
7	70	34.2	11.3	10.3	24.6	.25	.66	.39	1.690	1265	6.6	.53
8	156	38.9	11.3	9.8	25.9	.31	.57	.59	.970	1013	10.9	.72
9	157	33.1	10.1	8.6	23.7	.25	.45	.69	.652	900	14.0	.83
10	107	95.7	22.6	19.0	74.3	.22	.53	.69	.766	2010	26.3	.42
11	87	86.3	18.8	15.8	73.2	.20	.41	.77	.538	2150	19.2	.38
12	87	101.0	24.5	21.5	69.4	.31	.56	.59	.957	4275	29.3	.55
13	79	74.3	16.9	15.5	63.7	.20	.46	.73	.636	1640	24.4	.44
14	83	91.0	18.8	15.7	77.3	.20	.56	.73	.770	1240	26.6	.48
15	87	111.8	24.0	19.7	80.5	.28	.46	.79	.583	3220	24.6	.52
16	81	59.9	13.2	11.2	41.9	.30	.66	.55	1.210	903	24.3	.71
17	119	70.3	18.2	15.5	61.7	.19	.52	.67	.782	1925	22.0	.38
18	73	79.1	13.9	12.2	57.6	.27	.52	.73	.709	975	32.6	.81
19	110	88.3	22.7	19.5	72.9	.17	.47	.76	.625	2410	23.3	.38
20	74	59.0	13.2	11.1	51.8	.20	.47	.74	.631	845	16.9	.48
21	76	59.9	13.1	11.8	41.4	.31	.49	.73	.671	1280	27.1	.89
22	45	93.1	20.3	16.5	64.2	.31	.38	.84	.448	2210	22.9	.76
23	28	68.8	15.2	13.2	48.7	.29	.29	.88	.326	2540	26.0	.74
24	25	70.8	11.4	10.0	49.9	.29	.41	.67	.614	1295	37.4	.82
25	31	70.0	13.4	11.2	45.1	.36	.53	.69	.772	1860	31.6	.90

* See Table 3.1 for tree locations.

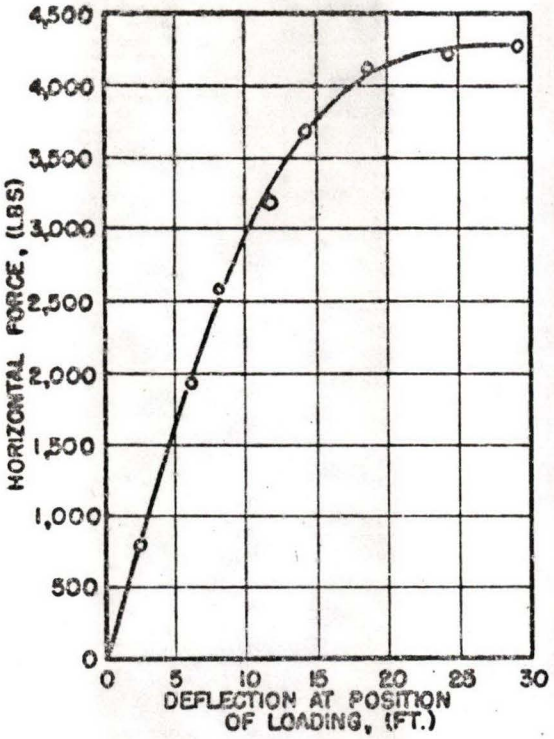

Fig. 4.1 Force-Deflection Curve for Tree Stem No. 12

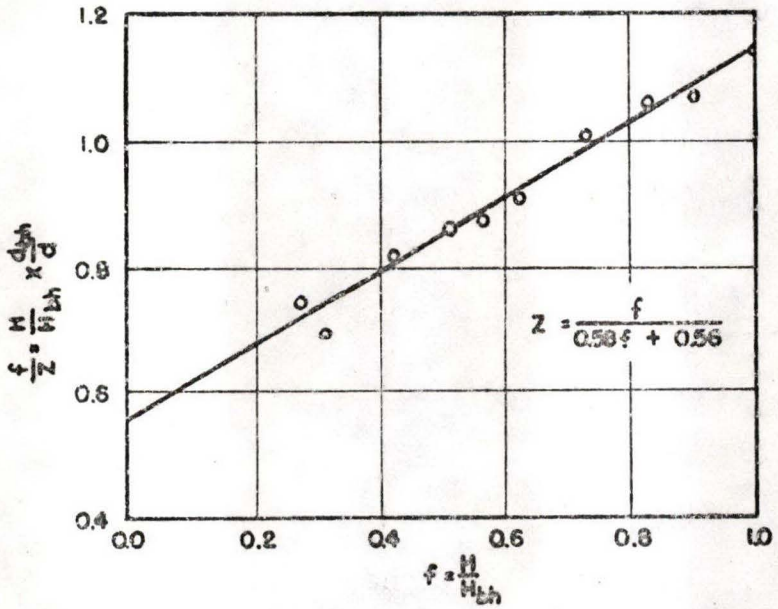

Fig. 4.2 Plot of z/f as a Function of f for Tree No. 12

TABLE 4.3

Values of Derived Stem Breakage Parameters

Column	1	2	3	4	5	6	7	8	9	10	11
Tree No.	k_a (Lb/Ft)	k_r (Lb/Ft)	$\bar{K}$	f_m	$\frac{s_m}{s_{bh}}$	s_{br} (Lb/Sq In.)	s_m (Lb/Sq In.)	$y_r(f_1)$ (Ft)	$\bar{Y}$	R_r (Lb)	$\bar{R}$
1	180	280	.643	1.00	1.00	2908	3016	15.30	1.40	4290	.573
2	460	505	.910	1.00	1.00	2667	2751	8.84	1.58	4470	.605
3	320	554	.578	1.00	1.00	1759	2215	15.15	1.32	8370	.465
4	518	1610	.322	1.00	1.00	5485	5485	4.41	2.61	7090	.487
5	360	1240	.289	1.00	1.00	1535	1653	6.75	2.15	8370	.299
6	146	234	.625	.39	1.21	6301	7107	5.25	2.85	1225	1.180
7	289	322	.900	.43	1.45	5087	5232	[illegible]	1.68	1260	1.002
8	150	229	.655	.75	1.01	3596	3596	5.06	2.15	1160	.875
9	183	207	.884	1.00	1.00	4162	4276	4.96	2.82	1030	.875
10	117	228	.513	.50	1.04	2727	2782	15.26	1.72	3479	.578
11	119	119	1.000	1.00	1.00	3820	4579	18.27	1.05	2174	.989
12	311	368	.845	.82	1.01	3411	3677	15.21	1.93	5597	.764
13	100	160	.625	.50	1.00	3162	3201	14.32	1.70	2291	.716
14	52	82	.634	.41	1.12	3156	3202	21.48	1.24	1761	.704
15	188	188	1.000	1.00	1.00	3340	4146	20.03	1.23	3766	.855
16	47	105	.448	.60	1.09	3484	3531	11.54	2.11	1212	.745
17	113	154	.734	.35	1.21	4311	4333	12.70	1.73	1956	.984
18	56	65	.862	1.00	1.00	3688	3791	19.29	1.69	1254	.778
19	160	204	.784	.37	1.08	3099	3089	17.99	1.30	3670	.657
20	63	84	.750	.48	1.00	3553	3593	12.55	1.35	1054	.802
21	71	172	.413	1.00	1.00	3938	3995	9.16	2.96	1576	.812
22	150	288	.521	1.00	1.00	3344	3923	13.94	1.64	4011	.551
23	194	286	.678	1.00	1.00	5296	6596	9.30	2.78	2655	.957
24	73	73	1.000	1.00	1.00	7854	8025	15.21	2.46	1112	1.160
25	109	164	.665	1.00	1.00	6984	7128	11.05	2.86	1807	1.030

TABLE 4.4

Equations Used in Calculating Derived Parameters in Table 4.3

Parameter	Equation	Remarks
k_a	2.6	Let $k_r = k_a$ R and $y(f_1)$ from Appendix B for small deflection
k_r	2.10	
$\bar{K}$		Ratio of k_a to k_r
f_m	2.5	
$\frac{s_m}{s_{bh}}$	2.4	Let $f = f_m$
s_{br}	2.4	Let $f = f_{br}$
s_m	2.4	Let $f = f_m$
$y_r(f_1)$	2.15	Let $\delta_m = \delta_r$
$\bar{Y}$		Ratio of $y_b(f_1)$ to $y_r(f_1)$
R_r	2.6	Let $R = R_r$ and $y(f_1) = y_r(f_1)$
$\bar{R}$		Ratio of R_b to R_r

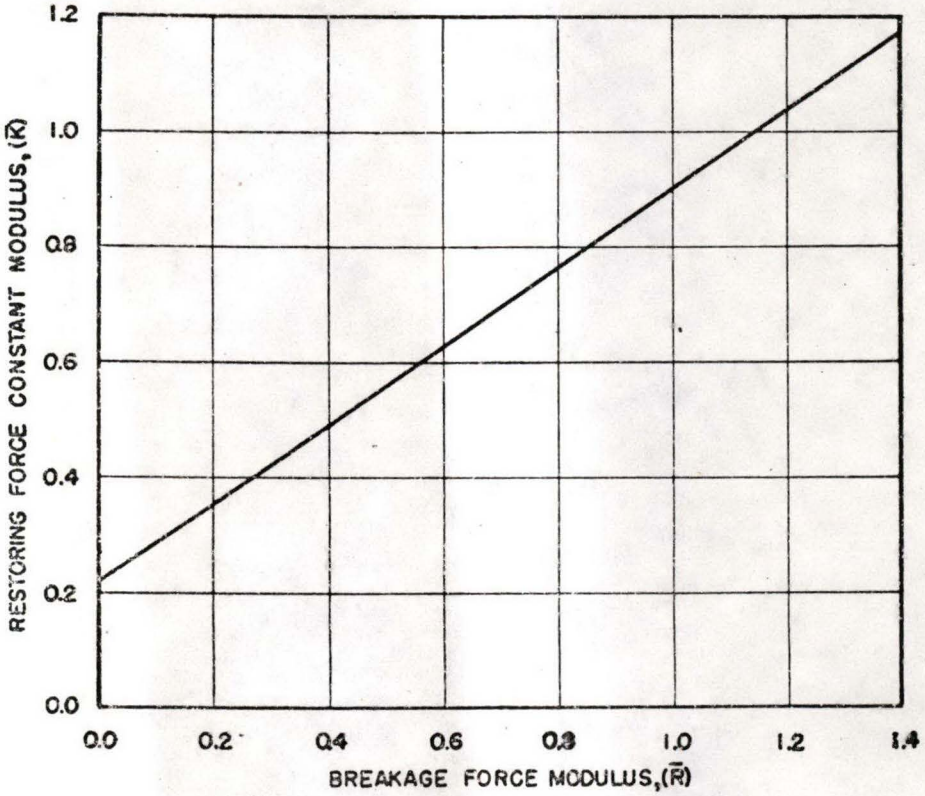

Fig. 4.3 Least Squares Regression of Restoring Force Modulus, $\bar{K}$, on Breakage Force Modulus $\bar{R}$. (The Coefficient of Correlation (0.59) is Highly Significant Using Students t-test.)

Statistical tests for homogeneity (Table 4.5) were made for three characteristics of the sample population:

Species - ponderosa pine and loblolly pine

Point of maximum stress - $f_m = 1$ and $f_m < 1$

Condition of the base - natural rooting and set in concrete

In each case difference between means was not significant at the 5 per cent level and the samples were considered to be drawn from a homogeneous population.

Cumulative frequency distributions of breakage moduli $\bar{Y}$ and $\bar{R}$ are shown in Figs. 4.4 and 4.5 as per cent of cases occurring which are equal to or larger than any chosen value. Chi-square tests confirmed the hypothesis that experimental values of $\bar{Y}$ and $\bar{R}$ were drawn from normally distributed populations defined by sample means and standard deviations. Cumulative normal frequency distributions were then calculated and the curves plotted in Figs. 4.4 and 4.5.

TABLE 4.5

Summary of Tests for Homogeneity of the Sample Population

Testing Significance of Differences Between Means of:	For Modulus	Total Degrees of Freedom	Mean Difference	Standard Error of Mean	Student's t		Conclusions
					Calculated	Tabular @ 5% Level	
Ponderosa pine	$\bar{K}$	23	0.072	0.128	0.56	2.07	(From
and	$\bar{R}$	23	0.175	0.117	1.50	2.07	(same
Loblolly pine	$\bar{Y}$	23	0.598	0.313	1.91	2.07	(population
Stems with $f_m = 1$	$\bar{K}$	23	0.045	0.095	0.47	2.07	(From
and	$\bar{R}$	23	0.073	0.093	0.78	2.07	(same
Stems with $f_m < 1$	$\bar{Y}$	23	0.243	0.243	1.00	2.07	(population
Natural rooting							(From
and	$\bar{K}$	23	0.072	0.128	0.56	2.07	(same
Set in concrete							(population

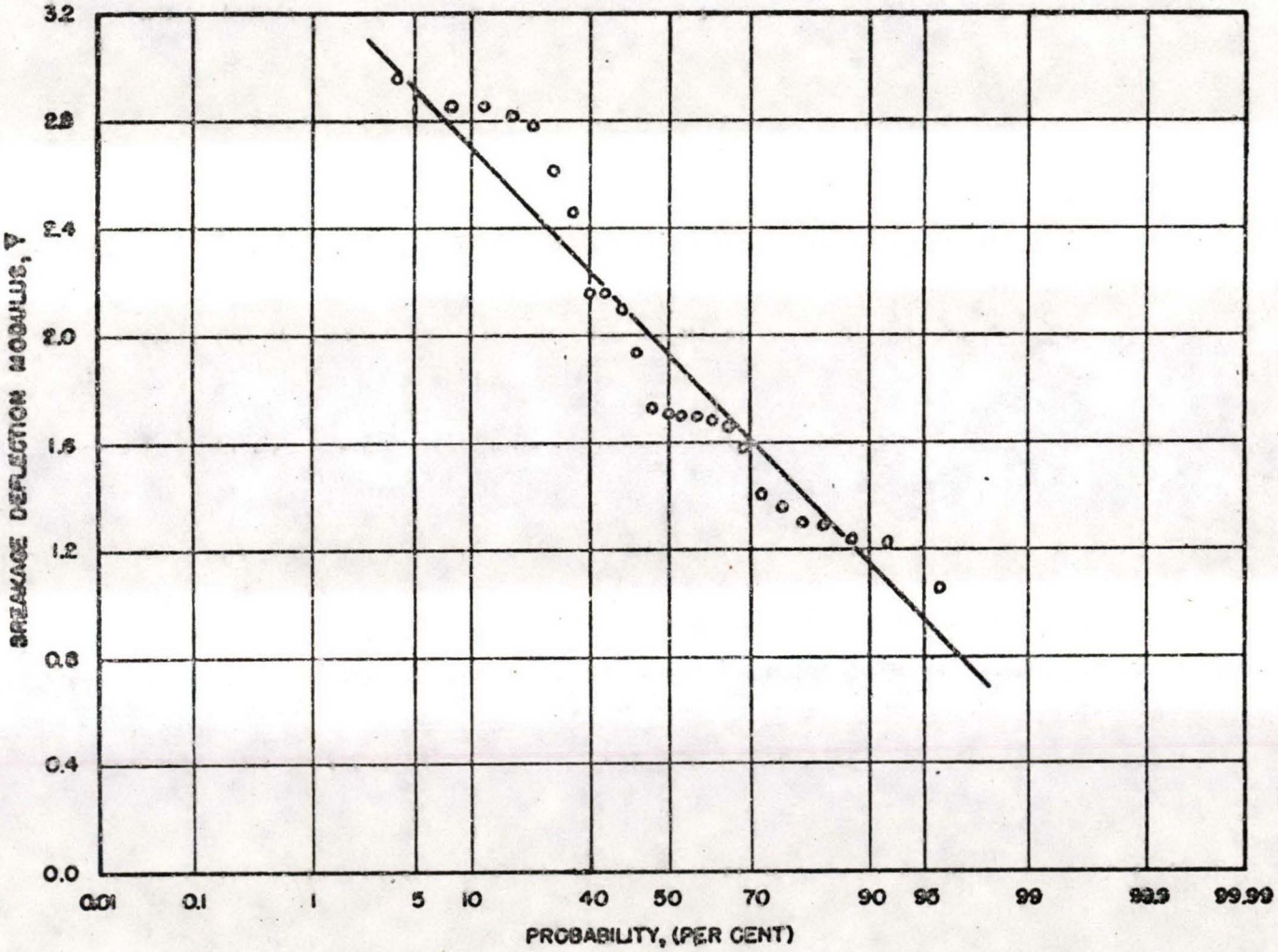

Fig. 4.4 Cumulative Normal and Actual Frequency Distributions--Breakage-Deflection Modulus $\overline{Y}$.

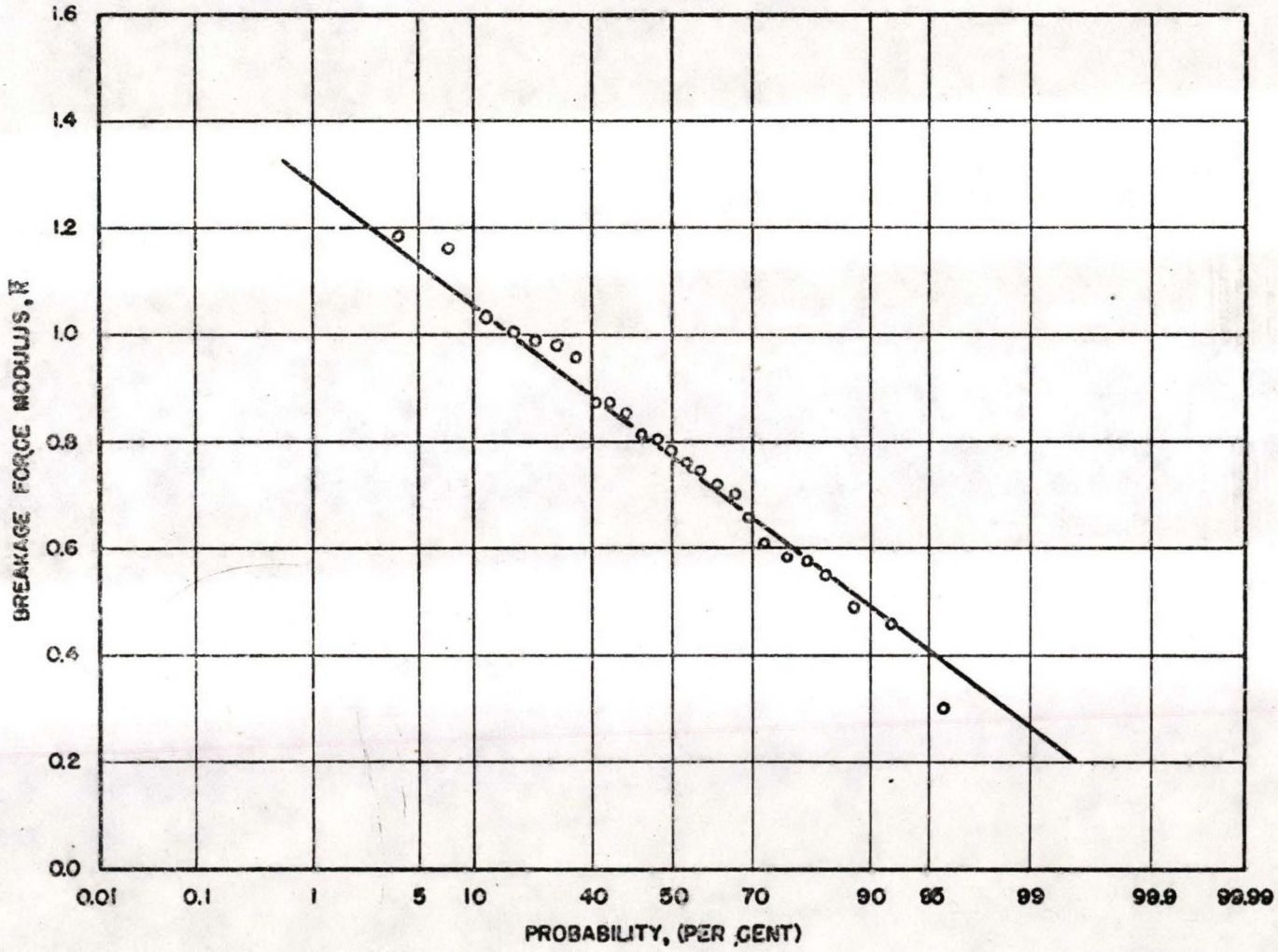

Fig. 4.5 Cumulative Normal and Actual Frequency Distributions--Breakage-Force Modulus $\bar{R}$

CHAPTER 5

DISCUSSION

The analysis presented in Chapter 2 allows prediction of forces and deflections required for static breakage of tree stems. Previous determinations of strength and related properties of wood [2] were made on sawed specimens selected for uniformity and absence of defect such as knot clusters. No work has been reported on prediction of stem failure of growing trees resulting from static loading.

For tree stems tested, stresses calculated for position of breakage, f_{br}, by Equation 2.4 were generally slightly lower than the calculated maximum stress. Average stress at the position of breakage was approximately 94 per cent of the calculated maximum stress and 70 per cent of the modulus of rupture for green sawed specimens (Table 4.2).

Examination of stems after breakage revealed that several failed at knot clusters, while others failed at an abrupt decrease in stem diameter. However, comparison of actual force required for breakage of tree stems and that required to break selected specimens of clear wood indicates a surprising strength of tree stems despite their heterogeneous structure.

Breakage Force and Deflection Moduli

Use of the dimensionless breakage force modulus $\overline{R}$, the breakage deflection modulus $\overline{Y}$, and the restoring force constant modulus $\overline{K}$ should permit grouping of test results independent of tree species, stem geometry, and position of loading. Field tests have indicated that such grouping is valid for different stem geometries and positions of loading, but only ponderosa and loblolly pine tree species have been investigated.

Structural irregularities found in tree stems account for the major part of variation in magnitude of breakage moduli. These irregularities include variations in mechanical properties of wood due to differences in growth rate, variations in soundness, injury, knot distribution, and variations in uniformity of stem form. In addition, the breakage deflection modulus is also affected by base firmness. In view of these many sources of variation, tree breakage must be considered on the basis of statistical probability. Because of the

---

[2] Markwardt and Wilson, op. cit.

diversity of sites and of base conditions of test trees, and the fact that statistical tests indicate that all trees are from the same population, application of probability based on the cumulative normal frequency distribution curves appears to be justified. Furthermore, it is believed that these normal-distribution curves apply to breakage force and deflection moduli of other coniferous species.

Some variation in these moduli is theoretically possible due to use of small deflection theory as a basis for computation of R_r, y_r, and k_r. Since the elastic equation is nonlinear under the condition of large deflections, it is not permissible to resolve the stem load into its components and treat the effect of each separately. Inasmuch as this analysis assumes that action of the vertical loading component is negligible, some variations in moduli are to be expected with changes in the angle of loading. The magnitude of this effect is under investigation.

Application of Force and Deflection Moduli to Breakage Probability

Application of this work should define the critical range of energy absorbed during breakage which lies between that energy which would break most tree stems and that which would leave most stems undamaged. For any tree with given diameter, height, stem form, and position of loading, force-deflection curves can be constructed to correspond to high and low breakage energy levels.

A tree postulated so that 95 per cent of trees in the population it represents will have lower values of both $\bar{Y}$ and $\bar{R}$ will require a relatively high breakage energy. Since the probability of these two moduli occurring simultaneously in one tree stem chosen at random is the product of the probabilities of their separate occurrences, at least 90 per cent of the trees in the population will require less breakage energy than the chosen stem. Similarly a tree can be postulated so that 95 per cent of trees in the population will have higher values of $\bar{Y}$ and $\bar{R}$, and therefore at least 90 per cent of the trees in the population will require more breakage energy.

Table 5.1 presents values of breakage moduli obtained from Figs. 4.4 and 4.5 which correspond to 95 and 5 per cent probability of their occurrence and therefore to the 90-per cent probability levels of breakage and non-breakage. These have arbitrarily been designated as covering the practical range of breakage energies.

Moduli values for 90-per cent probability of breakage and non-breakage given in Table 5.1 can be used to calculate corresponding force-deflection curves for any population of trees, all with identical diameter, height, stem form, and position of loading. Appendix C calculates a numerical example; resulting force-deflection curves are displayed in Fig. 5.1.

TABLE 5.1

Values of Breakage Moduli for 90-Per Cent Probability Levels of Breakage and Non-Breakage

Modulus	Value of Modulus	
	At least 90% [a] Will Break	At Least 90% [b] Will Not Break
$\bar{R}$	1.16	0.42
$\bar{Y}$	2.93	0.93
$\bar{K}$ [c]	0.94	0.48

a/ Corresponds to 95-per cent probability of occurrence, Figs. 4.4 and 4.5.
b/ Corresponds to 5-per cent probability of occurrence, Figs. 4.4 and 4.5.
c/ From Fig. 4.3.

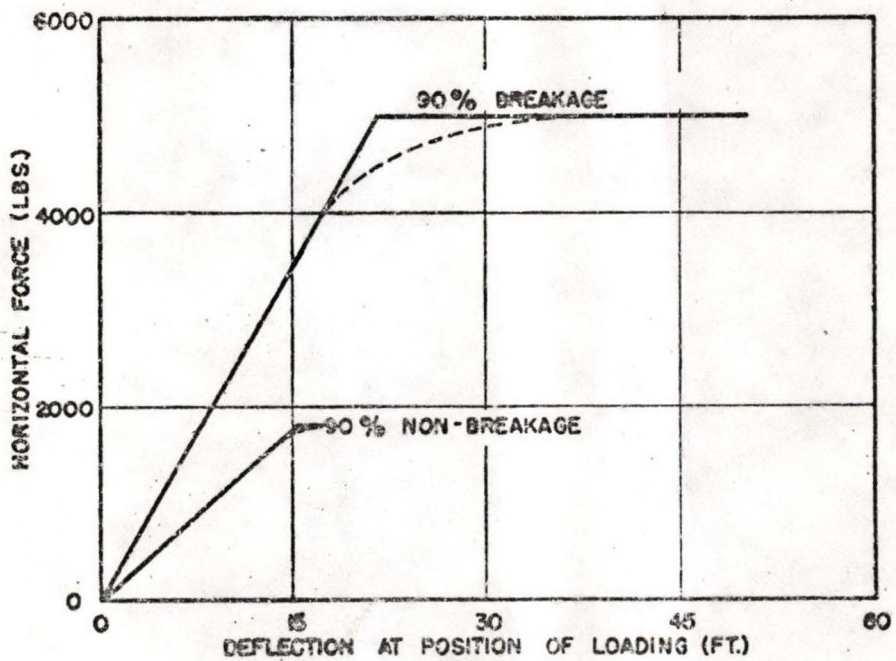

Fig. 5.1 Force-Deflection Curves for 90-Per Cent Probability Levels of Breakage and Non-Breakage. (From Calculations in Appendix C.)

The 90-per cent breakage force-deflection curve represents a given tree in a population 10/ defined by diameter, height, stem form, and position of loading such that amount of energy required to break this stem will break at least 90 per cent of those in the population.

The 90-per cent non-breakage force-deflection curve represents another tree from the same population 10/ such that the amount of energy required to break this tree will not damage at least 90 per cent of those in the population.

These two curves can be used to delineate the critical breakage energy range for the given tree population since they represent circumstances which are likely to occur at least 90 per cent of the time.

Since the calculation method used to obtain the curve in Fig. 5.1 does not determine the force at the proportional limit or define the elastic and plastic regions, a constant force in the plastic region is assumed. This assumption that the force is constant in the plastic region gives a slightly higher total energy than stems actually can absorb. Actual loading would more nearly follow the dotted curves.

Position of Stem Failure

Equation 2.4 indicates that stress distribution along a tree stem due to a single concentrated load varies with position of loading and stem form. Furthermore, position of stem failure can be expected to occur in the region where stress is near the maximum calculated by Equation 2.4, i.e. the region where $0.9 < s/s_m < 1$. A position of maximum stress may be predicted by Equation 2.5 from a known position of loading and stem-form factor. Figure 5.2 shows three typical types of stress distribution at breakage which result from three different positions of loading while holding stem form constant. Type A stress distribution is associated with loading near the top of stem. Type B and C distributions occur when loadings are at points lower down. Maximum stress for type A occurs near the point of loading, whereas for types B and C it occurs near or at the base of the stem.

Because of curvature of the stem and certain defects and the fact that the cross section may not be circular, stress distribution at breakage varies from that calculated by Equation 2.4. Approximate range of this variation is represented by the cross-hatched area in Fig. 5.2. Length "a" along the stem, in this figure, then, represents the critical length of stem where breakage may be expected for type A stress distribution. Lengths "b" and "c" are critical lengths for

10/ This population consists of all trees with stem characteristics given in Table C.1.

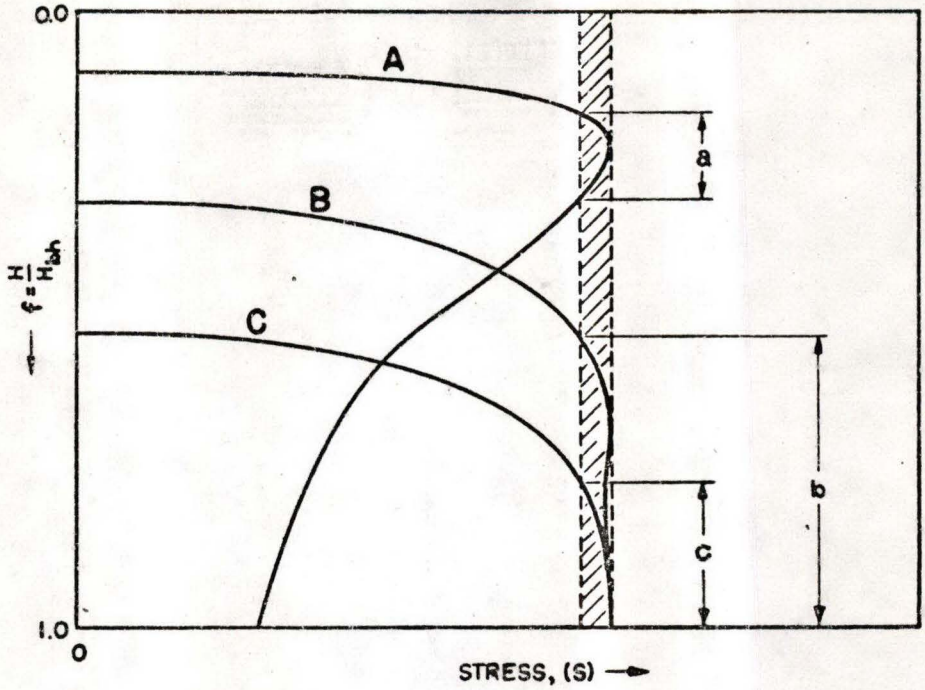

Fig. 5.2 Expected Stress Distribution for Three Different Positions of Loading

types B and C, respectively. When maximum stress occurs at the base, increased strength due to butt swell causes the position of breakage to move towards the top of "c".

In general, therefore, trees similar to those included in this study would be expected to break near the top as in "a" when they had a small crown concentrated at the top of the stem. Deeper crowned trees could be expected to break near or below the base of the crown, but not in the butt swell region near the ground.

Consideration must also be given to root strength and the possibility of uprooting. The fact that natural wind storms usually damage timber stands by uprooting may be attributed to high soil moisture from accompanying rains and to gustiness of winds during such storms. Periodic tree motion allows continuous loosening of roots, thus decreasing firmness of the base to a point where uprooting occurs. It appears, however, that without such weakening of roots, the root system of most pine trees offers considerably more resistance to failure than does the stem.

Field breakage tests under dynamic loading conditions 11/ indicate that the above discussion of position of failure also holds true for dynamic loading. In these tests, stem breakage due to blast loading occurred at or near the base of the crown.

These dynamic tests also showed that results of this study can be applied to calculation of blast damage to trees from atomic detonations, when suitable corrections for dynamic loading are applied to static force deflection curves.

11/ Forest Service, A.F.S.W.P. Operation SNAPPER 3.3 Final Report. Op. cit.

CHAPTER 6

CONCLUSIONS

1. This study establishes a method of correlating tree-stem breakage force and deflection data which is independent of tree stem geometry and position of loading, and is independent of the two species tested.

2. With equations presented and normal distribution curves established for force and deflection moduli, it is possible to construct a force-deflection curve for a tree stem of given diameter, height, stem form, and position of loading which corresponds to a particular breakage energy level.

3. Force and deflection at breakage vary approximately 300 per cent for apparently similar tree stems in a natural timber stand.

4. Position of stem breakage may be determined fairly accurately from stem form and position of loading.

5. Average extreme fiber stress at breakage of tree stems is approximately 70 per cent of the modulus-of-rupture value determined by standard static tests for green wood.

6. Ponderosa and loblolly pines are not likely to uproot by dynamic loading under low soil-moisture conditions.

7. Although this investigation was primarily concerned with breakage of ponderosa pine tree stems, the use of derived moduli in the analysis made it possible to include test data obtained for loblolly pine.

8. Breakage moduli normal distribution curves established by these tests may be used as an approximation for other coniferous species; however, this should be verified by making additional breakage tests on two or three more species.

APPENDIX A

DERIVATION OF RESTORING FORCE CONSTANT EQUATION

When the tangent to the elastic curve is small,[1/] the elastic curve equation becomes

$$\frac{d^2y}{dx^2} = \frac{Rx}{EI} \tag{A.1}$$

The deflection in the elastic region is then proportional to the applied force, and the relation of the applied force at f_1 in terms of the deflection at f_1 is

$$R = k_r\, y(f_1) \tag{A.2}$$

In Equation A.1, if x is taken as the distance along the stem measured from the point of force application, its expression in terms of total height of tree stem and position of loading is

$$x = H_{bh}(f - f_1) \tag{A.3}$$

Utilizing the stem form equation,

$$z = \frac{d}{d_{bh}} = \frac{f}{af + b}$$

an expression for the moment of inertia of the stem inside bark is written as

$$I = I_i\,(a + b)^4 \left(\frac{d}{d_{bh}}\right)^4$$

1/ For example, when $\frac{dy}{dx} < 0.1$, the error in Equation A.1 due to curvature would not exceed 4 per cent. See: P. G. Laurson and W. Cox. Mechanics of Materials. (2nd ed.), New York: John Wiley & Sons, Inc., 1949 (p. 157).

or

$$I = I_i (a + b)^4 \frac{f^4}{(af + b)^4} \qquad (A.4)$$

Substituting the expressions of I and x given in Equations A.4 and A.3 in Equation A.1 yields

$$\frac{d^2y}{dx^2} = \frac{R\, H_{bh}}{EI_i(a+b)^4} (f - f_1)\left(a + \frac{b}{f}\right)^4 \qquad (A.5)$$

and since $dx = H_{bh}df$ by differentiation of Equation A.3, it follows that

$$\frac{d^2y}{dx^2} = \frac{d^2y}{df^2} \frac{1}{H_{bh}^2}$$

and Equation A.5 becomes

$$\frac{d^2y}{df^2} = \frac{R\, H_{bh}^3}{EI_i(a+b)^4} (f - f_1)\left(a + \frac{b}{f}\right)^4$$

or

$$\frac{d^2y}{df^2} = \frac{R\, H_{bh}^3}{EI_i(a+b)^4} \left[a^4 f + a_1 + a_2 \frac{1}{f} + a_3 \frac{1}{f^2} + a_4 \frac{1}{f^3} - b^4 f_1 \frac{1}{f^4}\right] \qquad (A.6)$$

where

$$\begin{aligned} a_1 &= 4\, a^3 b - a^4 f_1 \\ a_2 &= 6\, a^2 b^2 - 4\, a^3 b\, f_1 \\ a_3 &= 4\, ab^3 - 6\, a^2 b^2\, f_1 \\ \text{and} \quad a_4 &= b^4 - 4\, ab^3\, f_1 \end{aligned} \qquad (A.7)$$

Integration of Equation A.6 gives

$$\frac{dy}{df} = \frac{R\,H b h^3}{EI_i(a+b)^4}\left[\frac{a^4 f^2}{2} + a_1 f + a_2 \ln f - a_3 \frac{1}{f} - \frac{a_4}{2}\frac{1}{f^2} + \frac{b^4 f_1}{3}\frac{1}{f^3} + C_1\right] \quad (A.8)$$

The constant of integration C_1 is determined for the condition that at $f = 1$, $\frac{dy}{df} = 0$; hence

$$C_1 = -\frac{a^4}{2} - a_1 + a_3 + \frac{a_4}{2} - \frac{b^4 f_1}{3} \quad (A.9)$$

Integrating Equation A.8 gives deflection y at f_1 as

$$y(f_1) = \frac{R\,H b h^3}{EI_i(a+b)^4}\left[\frac{a^4}{6} f^3 + \frac{a_1}{2} f^2 + a_2(f \ln f - f) - a_3 \ln f + \frac{a_4}{2}\frac{1}{f} - \frac{b^4 f_1}{6}\frac{1}{f^2} + C_1 f + C_2\right] \quad (A.10)$$

The constant of integration C_2 is determined for the condition that when $f = 1$, $y = 0$; hence

$$C_2 = -\frac{a^4}{6} - \frac{a_1}{2} + a_2 - \frac{a_4}{2} + \frac{b^4 f_1}{6} - C_1 \quad (A.11)$$

By equating Equations A.2 and A.10 with $\frac{b}{a} = c$ and with expressions for a_1, a_2, a_3, a_4, C_1, and C_2, and by suitable substitutions, a dimensionless quantity containing the restoring force constant, k_r, in terms of tree stem form factor c and position of loading is obtained:

$$\frac{k_r H_{bh}^3}{3EI_i} = \frac{(1+c)^4}{-f^3 + \left[3 + 6c\left(2 \ln \frac{1}{f_1} + 3\right) - 18c^2 - 6c^3 - c^4\right] f_1^2}$$

$$+ \left[c^4 + 8c^3 - 12c^2 \ln \frac{1}{f_1} - 8c - 1\right] f_1$$

$$+ \left[6c + 18c^2 + 6c^3\left(2 \ln \frac{1}{f_1} - 3\right) - 3c^4 + 1\right]$$

$$+ c^4 \frac{1}{f_1} \qquad \text{(A.12)}$$

Equation A.12 in functional form is

$$\frac{k H_{bh}^3}{3EI_i} = \phi (c, f_1) \qquad \text{(A.13)}$$

and its graph is presented in Fig. 2.2.

APPENDIX B

HORIZONTAL FORCE AND ARC-DEFLECTION FOR STATIC BENDING TESTS

Tree No.	Angle of Loading (Degrees)		Horizontal Force R (Lbs) and Arc-Deflection y (Ft)									
1	35	R	452	892	1345	1748	2029	2200	2298	2371	2408	2450*
		y	2.1	4.3	6.4	8.5	10.7	12.8	14.9	17.0	19.2	21.3*
2	25	R	506	998	1504	1956	2270	2462	2571	2652	2694	2700
		y	1.3	2.7	4.1	5.4	6.7	8.1	9.5	10.8	12.1	13.5
3	33	R	722	1424	2145	2788	3237	3510	3666	3783	3842	3900
		y	2.0	4.1	6.1	8.2	10.2	12.2	14.3	16.3	18.4	20.4
4	21	R	640	1263	1903	2474	2872	3114	3252	3356	3408	3450
		y	1.2	2.3	3.4	4.6	5.8	6.9	8.0	9.2	10.3	11.5
5	21	R	469	925	1394	1812	2104	2282	2383	2459	2497	2500
		y	1.4	2.9	4.4	5.8	7.2	8.7	10.2	11.6	13.0	14.5
6	19	R	301	428	552	728	1445					
		y	1.8	3.4	4.8	7.0	15.0					
7	19	R	395	577	800	1003	1265					
		y	1.6	2.8	4.0	5.3	6.6					
8	21	R	237	500	626	1013						
		y	2.0	4.0	5.0	10.9						
9	19	R	256	396	561	900						
		y	2.2	3.7	6.0	14.0						
10	43	R	461	909	1228	1594	1867	1969				
		y	3.6	7.9	11.0	16.7	21.6	24.0				
11	19	R	793	1535	1993	2150						
		y	6.4	11.2	15.3	19.2						
12	21	R	826	1943	2567	3175	3691	4105	4200	4282		
		y	2.3	6.0	8.3	11.4	14.3	18.8	24.6	29.2		

* Values in last column for each tree represent force and deflection at breakage.

Appendix B - Continued

Tree No.	Angle of Loading (Degrees)		Horizontal Force R (Lbs) and Arc-Deflection y (Ft)									
13	21	R	736	937	1099	1308	1464	1536	1642			
		y	7.2	9.8	12.4	14.7	18.1	21.0	24.4			
14	15	R	355	775	1016	1234	1217					
		y	7.8	15.0	20.0	25.8	27.4					
15	33	R	830	2087	2532	3231						
		y	4.4	10.9	14.0	24.6						
16	12	R	350	514	702	766	862	904				
		y	8.3	10.8	14.0	17.3	20.6	24.3				
17	15	R	471	864	1221	1615	1616	1924				
		y	4.2	7.4	11.3	14.9	17.9	22.0				
18	22	R	296	388	555	594	703	854	977			
		y	5.8	6.8	9.2	10.5	13.9	22.1	32.6			
19	25	R	367	996	1495	1780	2106	2417				
		y	2.4	6.2	9.4	12.1	16.6	23.3				
20	24	R	358	544	658	782	847					
		y	5.6	8.7	11.2	14.0	16.9					
21	12	R	121	326	530	637	775	877	1014	1178	1282	
		y	2.0	4.4	7.1	9.0	11.3	13.5	17.3	21.4	27.1	
22	27	R	207	823	1436	1702	1834	1823	2222			
		y	3.5	7.2	9.7	12.3	14.5	17.0	22.6			
23	29	R	240	1116	1423	1656	1886	2032	2258			
		y	1.3	4.8	7.5	9.6	11.7	14.6	17.8			
24	29	R	124	406	696	867	995	1099	1294			
		y	1.5	4.6	7.1	11.1	15.1	18.8	37.5			
25	24	R	401	642	843	1143	1310	1369	1484	1596	1613	1864
		y	3.1	5.0	8.1	10.0	13.2	15.4	18.4	22.0	24.6	31.5

APPENDIX C

NUMERICAL EXAMPLE, CALCULATION OF CRITICAL ENERGY RANGE

Table C.1 presents stem characteristics for the tree population selected as the sample for this calculation. Calculated population parameters based on these tree stem characteristics are given in Table C.2. Values of $y_r(f_1)$, R_r, and k_r from Table C.2 are combined with moduli values from Table 5.1 to obtain values of R_b, y_b, and k_a (Table C.3), used in plotting force-deflection curves for the two trees representing 90-per cent probability levels of breakage and non-breakage. These curves are plotted in Fig. 5.1.

TABLE C.1

Tree-Stem Characteristics

Species: ponderosa pine		
H_{bh}	height of stem above DBH	= 105 ft
d_{bh}	diameter outside bark at DBH	= 24 in.
d_i	diameter inside bark at DBH	= 20 in.
f_1	position of loading	= 0.30(73.5 ft above DBH)
c	stem form factor	= 0.75

TABLE C.2

Values of Parameters

Parameter	Equation No.	Value
f_m	2.5	1.00
$\frac{s_m}{s_{bh}}$	2.4	1.00
$y_r(f_1)$	2.15	17.5 ft
R_r	2.6	4,319 lbs
k_r	2.10	247 lbs/ft

TABLE C.3

Force-Deflection Values at Breakage for Trees Representing 90-Per Cent Probability Levels of Breakage and Non-Breakage

Factor	Equation	Value	
		At Least 90% Will Break	At Least 90% Will Not Break
R_b	$R_b = \bar{R}\, R_r$	5,010 lbs	1,814 lbs
y_b	$y_b = \bar{Y}\, y(f_1)$	51.3 ft	16.3 ft
k_a	$k_a = \bar{K}\, k_r$	233 lbs/ft	119 lbs/ft

NOMENCLATURE

a = constant in stem form equation

b = constant in stem form equation

$c = \frac{b}{a}$, stem form factor

C = distance from outer fiber to neutral axis

d = diameter along stem inside bark, in.

d_{bh} = stem diameter at breast height, in.

d_i = stem diameter inside bark at breast height, in.

E = modulus of elasticity, lbs/sq in.

$f = H/H_{bh}$, fractional height of stem measured from top of stem downward

f_{br} = position of stem breakage

f_m = position of maximum stress

f_l = position of loading

h = distance from point of loading to breast height, ft

H = height of stem measured from top of stem downward, ft

H_{bh} = height of stem above breast height, ft

I = moment of inertia inside bark, $in.^4$

I_{bh} = moment of inertia at breast height outside bark, $in.^4$

I_i = moment of inertia inside bark at breast height, $in.^4$

k_a = actual restoring force constant, lbs/ft

k_r = restoring force constant, lbs/ft

$\overline{K} = \frac{k_a}{k_r}$ = restoring force constant modulus

M = bending moment, lbs/ft

R = horizontal applied force, lbs

R_b = horizontal force at breakage, lbs

R_r = reference breakage force, lbs

$\overline{R} = \frac{R_b}{R_r}$ = breakage force modulus

s = extreme fiber stress, lbs/sq in.

s_{bh} = extreme fiber stress at breast height, lbs/sq in.

s_{br} = extreme fiber stress at position of stem breakage, lbs/sq in.

s_m = maximum extreme fiber stress, lbs/sq in.

S = modulus of rupture, lbs/sq in.

x = distance from point of loading, in.

$y(f_l)$ = stem deflection at point of loading, ft

$y_b(f_l)$ = deflection at breakage, ft

$y_r(f_l)$ = reference breakage deflection, ft

$\overline{Y} = \frac{y_b}{y_r}$ = breakage deflection modulus

$z = \frac{d}{d_{bh}}$, ratio of diameter of stem to diameter at breast height

δ = unit strain, in/in.

δ_{bh} = strain at breast height, in/in.

δ_m = maximum strain, in/in.

δ_r = reference strain, in/in.

ϕ = a function

ψ = a function